論文 / 著書情報
Article / Book Information

論題(和文)	
Title(English)	CYCLE-BY-CYCLE 3D ANALYSIS OF A FULL-SCALE VE DAMPER UNDER 100% SHEAR STRAIN
著者(和文)	LIANGQIJUN, 佐藤 大樹, OSABEL Dave M.
Authors(English)	Qijun Liang, Daiki Sato, Dave M Osabel
出典 / Citation	日本建築学会関東支部研究報告集, Ⅰ, , pp. 441-444
Citation(English)	, Ⅰ, , pp. 441-444
発行日 / Pub. date	2023, 2
権利情報	一般社団法人 日本建築学会

2022年度日本建築学会
関東支部研究報告集Ⅰ
2023年2月

CYCLE-BY-CYCLE 3D ANALYSIS OF A FULL-SCALE VE DAMPER UNDER 100% SHEAR STRAIN

構造ー振動

正会員 ○ LIANG Qijun *1　同 佐藤 大樹 *2
同 OSABEL Dave M. *3

Multi-layered viscoelastic (VE) damper, Sinusoidal loading
Finite element method, Heat generation, Heat transfer analysis

1. INTRODUCTION

1.1. Viscoelastic damper

Viscoelastic (VE) damper dissipates structural vibration through shear deformation of the viscoelastic material, then converts the absorb energy into heat. Hence, its temperature can significantly increase. Since it is sensitive to frequency and temperature, effect of heat generation and heat transfer must be considered.

Shown in Figures 1a and 1b are the force-deformation ($F_d - u_d$) and the force-velocity ($F_d - \dot{u}_d$) hysteresis curves, respectively, of a VE damper subjected to harmonic loading. Their slopes are the storage stiffness K'_d and damping coefficient C_d, respectively.

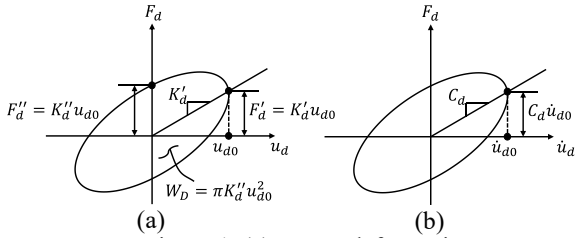

Figure 1. (a) Force–deformation and (b) force–velocity curves

1.2. Objective

The cycle-by-cycle three-dimensional (3D) analysis method had been proposed by Kasai et al[1], which utilized the linear modeling approach[2] to estimate two-layered VE dampers subjected to 50% peak shear strain sinusoidal loading. The said 3D analysis has shown excellent accuracy.

Since it is necessary to evaluate the accuracy of the cycle-by-cycle 3D analysis method on larger scale dampers and subject to larger peak shear strain, Osabel et al[3] extended the method to a six-layered VE damper subjected to 75% peak shear strain sinusoidal loading. Their 3D analysis fit well with experimental results, which indicates that the VE damper still behaved under the linear constitutive rule.

As VE damper can be subjected to peak shear strain of more than 75%, this study investigated full-scale eight-layered VE damper subjected to peak shear strain of 100%.

2. VE DAMPER EXPERIMENT

This chapter presents the deformation-controlled loading experiment on VE damper from the study of Kasai et al[4].

2.1. Test specimen and setup

Figure 2 shows the eight-layered VE damper used in the experiment. The damper is symmetrical in the $XY-$ and $XZ-$ planes (C-axis and L-axis). The 3M-ISD111 type VE material used in this damper has the following properties: shear modulus $G = 3.92$ N/cm^2, fractional derivative order $\alpha = 0.558$, temperature sensitive constants $a_{ref} = 0.000056$ and $b_{ref} = 2.10$ at reference temperature θ_{ref} = 20℃, $p_1 = 14.06$ and $p_2 = 97.32$.

The dimensions of VE damper test specimen are: length l =3946.6 mm, thickness of one VE slab d_V =8 mm, total shear area A_s =13120 cm^2, number of laminations n_V =8, shape factor A_s / d_V =16400 cm.

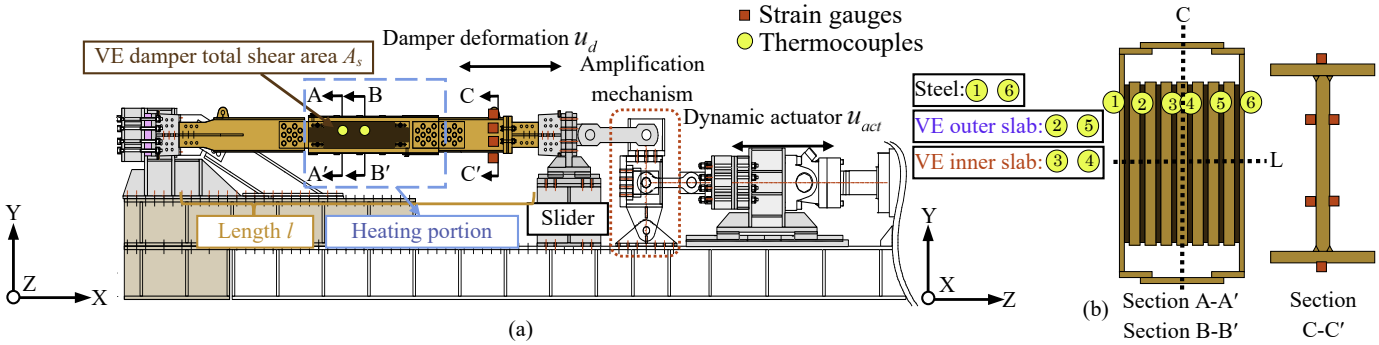

Figure 2. (a)Test setup of VE damper, (b)locations of thermocouples and strain gauges

Temperature θ inside the damper (VE slabs) and on the steel surfaces at Sections A-A′ and B-B′ (Figure 2b), and ambient temperature θ_a were measured continuously at time-increment of 0.026 seconds during the application of loading. The VE damper was heated to 22 °C by enclosing it by electric blanket (heating portion shown in Figure 2a). Note that the blanket was removed before loading started.

The damper deformation u_d was measured using linear displacement transducers. Damper force F_d was calculated using the measured strains at Section C-C′ (Figure 2b).

2.2. Deformation-controlled loading

Deformation-controlled loading was applied by the dynamic actuator. To attain the desired dynamic damper deformation, amplification mechanism was used (Figure 2a). Ideally, the damper deformation u_d should be twice that of the actuator deformation u_{act}. However, u_{act} was not effectively translated to u_d due to high resistive force by the VE damper. Despite this, the measured u_d will be used as input wave for the analysis in Chapter 3, which has the following properties: duration $t_a = 1200$ s, frequency $f_r = 0.25$ Hz.

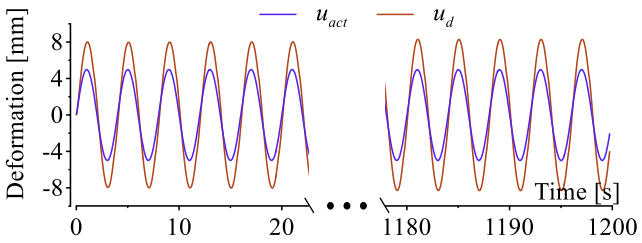

Figure 3. Test data of u_{act} vs. u_d

2.3. Experimental results

Figure 4 shows the average temperatures for VE slabs at Sections A-A′ and B-B′ (Figure 2b), i.e., "Steel" = average of thermocouples 1 and 6, "VE outer slab" = average of thermocouples 2 and 5, and "VE inner slab" = average of thermocouples 3 and 4.

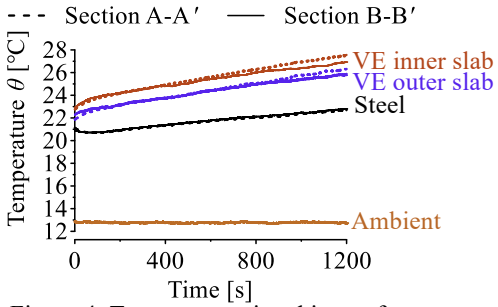

Figure 4. Temperature time history from test

Damper temperature increases after loading started and is almost the same at the respective VE slab in different sections. VE slabs have higher temperatures than steel because they have low thermal conductivity, thereby, accumulate heat. VE inner slab has the higher temperature than that of VE outer slab because it has the least heat transfer to the surrounding air and steel.

As for the storage stiffness K'_d and damping coefficient C_d, they are calculated using the least squares method, i.e.,

$$K'_d = \frac{n\sum\left(u_d^{(i)} \cdot F_d^{(i)}\right) - \sum u_d^{(i)} \sum F_d^{(i)}}{n\sum\left(u_d^{(i)}\right)^2 - \left(\sum u_d^{(i)}\right)^2}, \text{ and} \quad (1)$$

$$C_d = \frac{n\sum\left(\dot{u}_d^{(i)} \cdot F_d^{(i)}\right) - \sum \dot{u}_d^{(i)} \sum F_d^{(i)}}{n\sum\left(\dot{u}_d^{(i)}\right)^2 - \left(\sum \dot{u}_d^{(i)}\right)^2}, \quad (2)$$

where n = number of data. The K'_d and C_d from the test will be shown in Figure 9 of Chapter 3.

3. CYCLE-BY-CYCLE 3D ANALYSIS

The VE damper tested in Chapter 2 will be analyzed using the 3D-FEM proposed by Kasai et al[1].

3.1. Overview of the 3D-FEM analysis

Due to page limitation, only the flowchart of the 3D-FEM analysis[1] is shown in Figure 5. Using the initial temperature θ_j, the material property (the storage shear modulus G'_j and the loss factor η_j) of each VE element j is calculated adopting the temperature-frequency dependency rule proposed by Kasai et al[2]. The VE damper is set to maximum deformation u_{d0} to obtain the reaction force F'_d. The energy dissipated per cycle W_j, which corresponds to the area of the force-deformation hysteresis (Figure 1a), can be estimated.

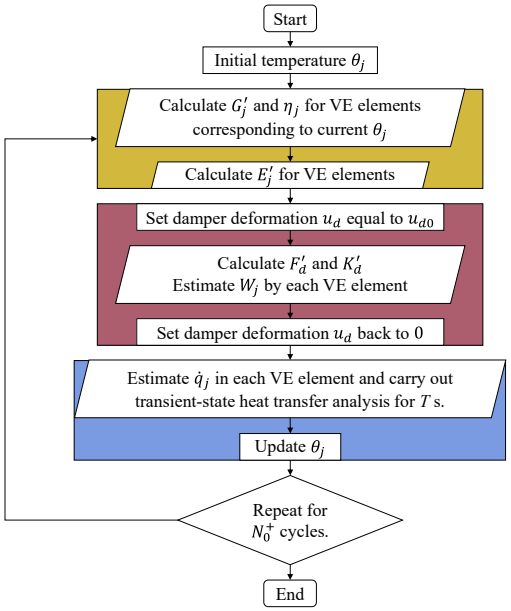

Figure 5. Flowchart of the 3D-FEM analysis

The K'_d, loss stiffness K''_d and C_d for the corresponding cycle n_c can be approximated as:

$$K'_d = F'_d / u_d, \quad K''_d = \left(\sum\nolimits_j W_j\right) / \left(\pi u_{d0}^2\right), \quad \text{(3a, b)}$$

$$C_d = K''_d / \left(2\pi f\right). \quad (4)$$

The force-deformation hysteresis curve can be plotted using the K'_d and K''_d (Eq. 3), i.e.,

$$F_d = K'_d u_d \pm K''_d \sqrt{u_{d0}^2 - u_d^2}. \quad (5)$$

Then, u_d is set back to zero. Using W_j to calculate the rate of heat generation $\dot{q}_j$ per unit volume V_j. The 3D transient-state heat transfer analysis is then carried out to update the element temperature θ_j. The above procedure for the static and transient analysis is repeated for N_0^+ cycles. Ambient temperature θ_a was assumed to be constant at 12.7 °C.

Since the damper is symmetrical in C- and L-axes (Figure 2b), a quarter of the damper was modeled. The 3D model and the initial temperature distributions are shown in Figure 6. The model was subjected to static load (corresponding to the deformation-controlled loading of the test, Figure 7) along the x – direction. The load was applied at one end of the model so that it will be collinear with the reaction force at the other end, simulating purely axial loading. In order to simulate the effect by electric blanket, the initial temperature of both end was 12.7 °C, while the surfaces of the steel were 21.0 °C, and inside damper was 22.0 °C.

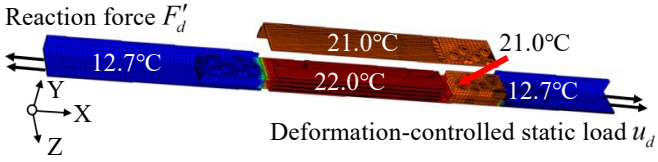

Figure 6. The 3D model and initial temperature distribution

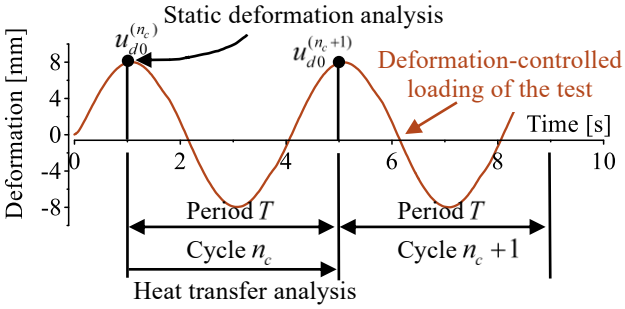

Figure 7. Cycle-by-cycle static and heat transfer analysis

Additional VE material properties are: thermal conductivity of VE and steel are $\kappa_{VE} = 0.188$ N/s/ °C and $\kappa_{steel} = 0.188$ N/s/°C, respectively; specific heat capacity of VE and steel are $s_{VE} = 18.70\times10^4$ N·cm/kg/°C and $s_{steel} = 46.63\times10^3$ N·cm/kg/°C, respectively; mass density of VE and steel are $\rho_{VE} = 1.0\times10^{-3}$ kg/cm^2 and $\rho_{steel} = 7.8\times10^{-3}$ kg/cm^2.

3.2. Obtaining ideal heat transfer coefficient α_c

The value of heat transfer coefficient α_c, which describes the rate of heat dispersion to surrounding air, depends upon many air flow parameters as well as air-exposed surface roughness of VE damper. To simplify the analysis, only one value of α_c was assigned to all air-exposed surfaces and assumed to be constant throughout the loading. The α_c value is determined in this section by trial-and-error approach.

Figures 8 and 9 show the temperature θ, storage stiffness K_d' and damping coefficient C_d obtained from analysis using trial values of α_c (= 0, 5, and 10 N/s/m/ °C), respectively. The temperatures of VE slabs are almost the same in all three cases, indicating less sensitivity to α_c value.

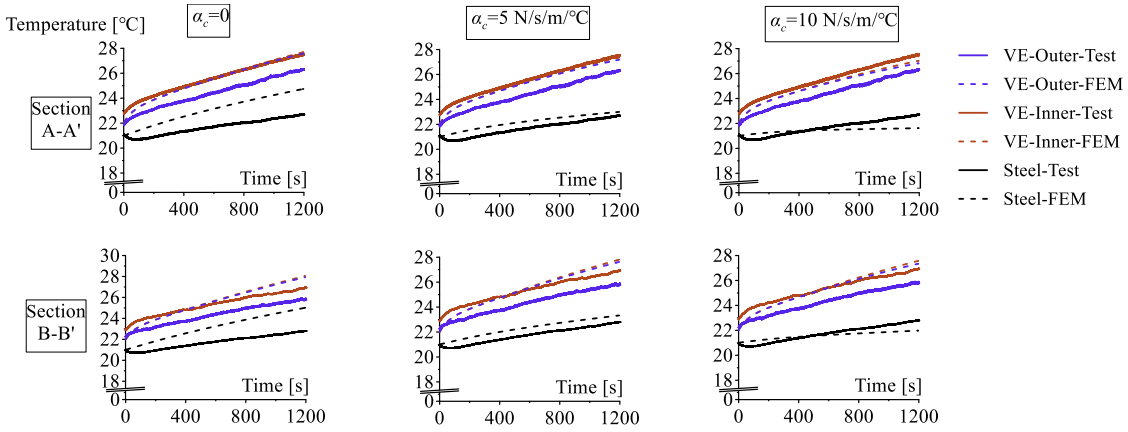

Figure 8. Temperature results from analysis for trial values of α_c

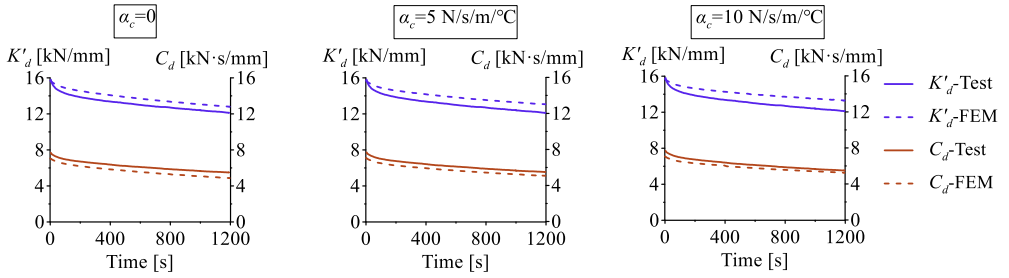

Figure 9. The Storage stiffness K_d' and damping coefficient C_d for trial values of α_c

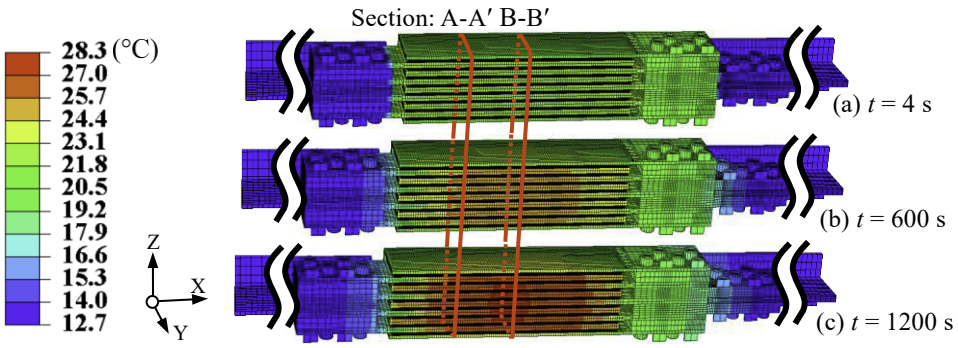

Figure 10. Temperature distribution: 3D-FEM transient state (α_c = 5 N/s/m/ °C)

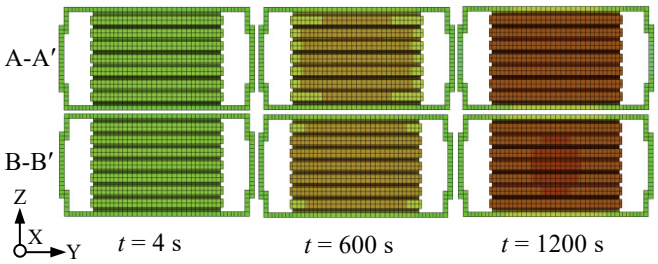

Figure 11. Temp distribution in Sections A-A′ and B-B′

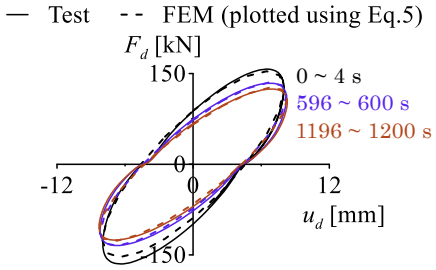

Figure 12. $F_d - u_d$ curves (α_c = 5 N/s/m/ °C)

On the other hand, the steel temperature shows higher sensitivity to α_c value, which is higher in lower α_c case. Analysis without considering heat dispersion to air (α_c = 0) has significantly larger steel temperature than the test, which is not good enough to simulate the test. Hence, effect of heat transfer to air must be considered. Steel temperatures from analysis using α_c = 5 N/s/m/ °C are closer to the measured temperatures than those using α_c = 10 N/s/m/ °C .

Meanwhile, the K_d' and C_d appear to be almost the same for all trial values of α_c . Hence, the α_c value adopted as the most appropriate value is 5 N/s/m/ °C .

3.3. Simulation results using α_c = 5 N/s/m/°C

Temperature distributions from the 3D-FEM analysis using α_c = 5 N/s/m/ °C at different time instances are shown in Figures 10 and 11. From initial temperature value of 21.0 °C , the surface steel temperature rises to at least 21.8 °C .

Meanwhile, from initial temperature value of 22.0 °C , the inside damper temperature rises to a maximum of 28.3 °C . The temperature in the VE material is significantly larger than that of the steel at the end of loading (t = 1200 s).

Figure 12 shows the $F_d - u_d$ hysteresis curves in the beginning (0 ~ 4 s), middle (596 ~ 600 s), and the end (1196 ~ 1200 s) of the loading, respectively, obtained from the analysis and the test. As shown, the results from the analysis are matching well with the test.

4. Conclusions

This study numerically investigated the eight-layered VE damper subjected to 100% peak shear strain sinusoidal wave by using the previously proposed finite element analysis method[1] utilizing linear modeling approach[2].

The analysis results matched well with the test, accurately predicting the VE damper dynamic properties.

Temperature on steel surfaces was found to be more sensitive to varying trial values of heat transfer coefficient α_c as compared to that of inner parts of such full-scale VE damper. From the above, the linear modeling approach[2] still work for VE damper under 100% peak shear strain.

For future study, the accuracy of linear modeling approach[2] for VE damper under 200% peak shear strain will be investigated.

References

[1] Kasai K, Sato D, Huang YH. Analytical methods for viscoelastic damper considering heat generation, conduction and transfer under long-duration cyclic load. J Struct Constr Eng 2006; 599:61–9 (In Japanese).

[2] Kasai K, Teramoto M, Okuma K, Tokoro K. Constitutive rule for viscoelastic materials considering temperature and frequency sensitivity (Part 1: Linear model with temperature and frequency sensitiveness). J Struct Constr Eng, AIJ. 2001; 543:77-86 (In Japanese).

[3] Osabel Dave M, Sato D., Kasai K. Study of Full-Scale Multi-Layered Viscoelastic Dampers under Long-Duration Harmonic Loading (Part 3: Characteristics of a Viscoelastic Damper under Different Loading Conditions). Summaries of technical papers of annual meeting, pp. 751-752

[4] Sato D, Kasai K, Sakaibara N, (2014). Experiment of Full-Scale Viscoelastic Damper and Analysis due to Change in Dynamic Characteristics under Long-Period Ground Motion. Architectural Institute of Japan, Vol. B-2, pp. 1009-1010.

*1 東京工業大学 研究生

*2 東京工業大学 准教授・博士（工学）

*3 東京工業大学 博士研究生

* Research Student, Tokyo Institute of Technology *1

* Associate Professor, FIRST, Tokyo Institute of Technology, Dr. Eng.*2

* PhD researcher, Tokyo Institute of Technology, PhD.*3